

# Effects of compressive residual stress on short fatigue crack growth in a nickel-based superalloy

Li, Hangyue; Sun, Hailin; Bowen, Paul; Knott, John

DOI:

[10.1016/j.ijfatigue.2017.11.010](https://doi.org/10.1016/j.ijfatigue.2017.11.010)

License:

Creative Commons: Attribution-NonCommercial-NoDerivs (CC BY-NC-ND)

*Document Version*

Peer reviewed version

*Citation for published version (Harvard):*

Li, H, Sun, H, Bowen, P & Knott, J 2018, 'Effects of compressive residual stress on short fatigue crack growth in a nickel-based superalloy', *International Journal of Fatigue*, vol. 108, pp. 53-61.

<https://doi.org/10.1016/j.ijfatigue.2017.11.010>

[Link to publication on Research at Birmingham portal](#)

## General rights

Unless a licence is specified above, all rights (including copyright and moral rights) in this document are retained by the authors and/or the copyright holders. The express permission of the copyright holder must be obtained for any use of this material other than for purposes permitted by law.

- Users may freely distribute the URL that is used to identify this publication.
- Users may download and/or print one copy of the publication from the University of Birmingham research portal for the purpose of private study or non-commercial research.
- User may use extracts from the document in line with the concept of 'fair dealing' under the Copyright, Designs and Patents Act 1988 (?)
- Users may not further distribute the material nor use it for the purposes of commercial gain.

Where a licence is displayed above, please note the terms and conditions of the licence govern your use of this document.

When citing, please reference the published version.

## Take down policy

While the University of Birmingham exercises care and attention in making items available there are rare occasions when an item has been uploaded in error or has been deemed to be commercially or otherwise sensitive.

If you believe that this is the case for this document, please contact [UBIRA@lists.bham.ac.uk](mailto:UBIRA@lists.bham.ac.uk) providing details and we will remove access to the work immediately and investigate.

## Accepted Manuscript

Effects of compressive residual stress on short fatigue crack growth in a nickel-based superalloy

H.Y. Li, H.L. Sun, P. Bowen, J.F. Knott

PII: S0142-1123(17)30436-X  
DOI: <https://doi.org/10.1016/j.ijfatigue.2017.11.010>  
Reference: JIJF 4505

To appear in: *International Journal of Fatigue*

Received Date: 8 June 2017  
Revised Date: 16 November 2017  
Accepted Date: 17 November 2017

Please cite this article as: Li, H.Y., Sun, H.L., Bowen, P., Knott, J.F., Effects of compressive residual stress on short fatigue crack growth in a nickel-based superalloy, *International Journal of Fatigue* (2017), doi: <https://doi.org/10.1016/j.ijfatigue.2017.11.010>

This is a PDF file of an unedited manuscript that has been accepted for publication. As a service to our customers we are providing this early version of the manuscript. The manuscript will undergo copyediting, typesetting, and review of the resulting proof before it is published in its final form. Please note that during the production process errors may be discovered which could affect the content, and all legal disclaimers that apply to the journal pertain.



## Effects of compressive residual stress on short fatigue crack growth in a nickel-based superalloy

H.Y. Li<sup>a,\*</sup>, H.L. Sun<sup>a,1</sup>, P. Bowen<sup>a</sup> and J.F. Knott<sup>a</sup>

*School of Metallurgy and Materials, College of Engineering and Physical Science, The University of Birmingham, Edgbaston, Birmingham B15 2TT, United Kingdom*

### Abstract

The effects of compressive residual stress on short fatigue crack growth in Inconel 718 have been investigated. Using two different indentation procedures, controlled plane-strain compressive residual stress fields were applied to short through-thickness cracks, which had been generated by machining away wakes of long cracks that had been grown down to threshold levels at a stress ratio of 0.1. Short fatigue crack growth tests were conducted at stress ratios of 0.1 and 0.7. At a stress ratio of 0.1, the residual stress-free testpieces demonstrated typical short fatigue crack growth behaviour, indicated by a reduction of threshold value and increases in fatigue crack growth rates compared to those of long fatigue cracks. A significant decrease in short crack growth rates was observed within the compressive residual stress region of indented testpieces, together with an increase of threshold values. At a high stress ratio of 0.7, any similar decrease in rate is barely observable. This indicates that the effects of compressive residual stress on short fatigue crack growth are monotonic in sign and could perhaps be simulated by a crack closure approach similar to that applied for long fatigue cracks. However the superposition principle which incorporates the compressive residual stress as a negative stress intensity factor, despite many successful applications to long fatigue cracks, is found to be inappropriate here. Hence one should be cautious when extending such a methodology to short fatigue cracks as it may result in optimistic life estimations.

**Key words** Residual stress, fatigue threshold, short fatigue crack growth, superposition principle

\*Corresponding author: Hangyue Li  
Telephone: +44 121 4142880  
Fax: +44 121 4147468  
Email: [h.y.li.1@bham.ac.uk](mailto:h.y.li.1@bham.ac.uk)  
<sup>1</sup>Present address: Miba Coating Group, Droitwich, Worcestershire WR9 9AS, UK

## 1. Introduction

Residual stress can be generated unintentionally in engineering components by manufacturing and fabrication processes such as forging, rolling, machining or welding. There are also surface mechanical processes such as shot peening which are intentionally applied to introduce beneficial compressive residual stresses into the surface layers of components. Shot peening has been extensively used in some critical components such as aero-engine rotor discs. The beneficial effects of shot peening in prolonging fatigue life and increasing fatigue strength have long been recognised [1]. Due to the high magnitude of compressive residual stress produced in the surface layer, crack initiation from the surface of the component is impeded. It is possible for cracks to be initiated internally: these are more weakly affected by the surface residual stress. Another possibility is that small cracks initiate from the surface due to the increased roughness induced by shot peening and grow within the compressive layer, but at rates reduced by the presence of residual stress. Depending on the applied stress range and geometry, they may even arrest. Early small crack growth behaviour in the presence of a residual stress field is not fully understood, although a considerable amount of work has been dedicated both to the “small crack growth effect” (without residual stress) and to the effect of residual stress on long fatigue crack growth. Such early small crack growth behaviour may contribute to the majority of the total fatigue life and hence it can be of great importance to structural analysis and lifing of components [2].

The work to study the influence of residual stress on fatigue crack growth has been mainly conducted for long fatigue cracks in long-range, low-magnitude residual stress fields. A superposition principle is often adopted. In such an approach, the influence of residual stress is converted to a stress intensity factor (SIF),  $K_r$ , and added on to the stress intensity factor result from the applied loading,  $K$ , to yield an “effective stress intensity factor”,  $K'$  and an “effective stress ratio”,  $R'$  [3]

$$R' = \frac{K'_{\min}}{K'_{\max}} = \frac{K_{\min} + K_r}{K_{\max} + K_r} \quad (1)$$

and

$$\Delta K' = K'_{\max} - K'_{\min} = (K_{\max} + K_r) - (K_{\min} + K_r) = \Delta K \quad (2)$$

where  $K_{\max}$ ,  $K_{\min}$  and  $K_r$  denote the values of SIF at the maximum applied load, the minimum applied load and that due to residual stress respectively. The growth rates are then interpreted using the crack growth laws generated with conventional laboratory testpieces free of residual stress [4]

$$\frac{da}{dN} = \frac{C(\Delta K)^m}{(1-R')K_c - \Delta K} \quad (3)$$

where  $C$  and  $m$  are constants, and  $K_c$  is the critical  $K$  value of fracture. The role of residual stress is thus not to change the SIF range but to add to the mean stress and to alter the effective stress ratio. Compressive residual stress reduces the effective  $R'$  ratio and hence may decrease the fatigue crack growth rate.

Another method is to use the “effective stress intensity factor range” concept first proposed by Elber [5]. This concept considers that crack closure occurs during part of the dynamic load range. If the effective stress intensity factor range is taken to represent the opening portion of SIF range, i.e.

$$\Delta K_{eff} = K_{\max} - K_{op} \quad (4)$$

where  $K_{op}$  is the measured crack opening stress intensity factor, then fatigue crack growth can be described by the equation,

$$\frac{da}{dN} = C(\Delta K_{eff})^m \quad (5)$$

which is now independent of stress ratio and crack size. In this approach, the effects of a residual stress field are incorporated by a change in the crack opening stress intensity factor. The approach is attractive as (5) can be determined easily by conducting fatigue crack growth tests at high stress-ratio on stress-free samples, and crack-opening response can be measured experimentally. Indeed such research has attracted intensive experimental and numerical assessments without residual stress, effects of crack growth regime,  $R$  ratio and crack size have all been studied. Effects of residual stress on crack closure is less well studied but it is generally understood that tensile residual stress reduces

the amount of crack closure (increasing  $\Delta K_{eff}$ ) and compressive residual stress has the opposite effect. A simple treatment of this approach is to assume that cracks open at a zero SIF under the combined influence of applied and residual stress. For  $(K_{min} + K_r) > 0$

$$\Delta K_{eff} = K'_{max} - K'_{min} = (K_{max} + K_r) - (K_{min} + K_r) = \Delta K \quad (6)$$

and now influence of residual stress on fatigue crack growth is minimal or absent. Whereas for  $(K_{min} + K_r) < 0$  (usually for the cases of compressive residual stresses)

$$\Delta K_{eff} = K'_{max} - 0 = (K_{max} + K_r) - 0 = K_{max} + K_r \quad (7)$$

The influence of residual stress now can be represented with “ $K_r$ ”. Indeed this has been confirmed to be the case for long fatigue cracks growing through a compressive residual stress field introduced by indentation [6].

It seems that quantifying the influence of residual stress can be dealt with largely by calculation of SIF generated by the residual stress field. The most convenient way to make such a calculation employs a weight function [7], which requires only the knowledge of the original crack-free residual stress distribution. Such approaches have been adopted extensively and are found to provide a reasonable estimation for long fatigue crack growth in a long range existing residual stress field of low magnitude which does not change sign. Despite the simplicity of the superposition methodology, it has been suggested for example, by Knott [8] that its applicability needs to be checked experimentally. There are complications which may invalidate such an approach. such as partial closure (crack surfaces closing at some distance behind the tip). Partial closure can occur typically for a crack immersed in a stress field where the sign changes, with the tip located in the tensile zone [9]. It is anticipated that such effects could be much more significant for the case of short fatigue crack growth within residual stress fields of high magnitude and large gradient, and it is not clear whether the methodology can be extended to short fatigue cracks. Here, the SIFs due to residual stress are of similar magnitude to those resulting from the applied stress, but change rapidly over short distances, and could possibly induce transient closure.

Only a few work have been reported relating to such subject. Lacarac et al. [10] studied fatigue crack growth from cold expanded holes in aluminium plates where a decrease in fatigue crack growth rates

in cold-expanded specimens was confirmed to be associated with increased stress required for crack opening due to the presence of compressive residual stress, compared to a similar hole not subjected to cold-expansion. However, the residual stress distributions and resultant SIFs were not provided. By using a 3D weight function method, Gao and Wu [11] calculated the SIFs for a shot peening residual stress distribution acting on small cracks located at the root of a notch surface. When added to the SIFs of the applied stress, again calculated using a weight function, normal small crack growth behaviour was observed. Their study supports the extension of the superposition principle into the small crack growth regime and suggests solving the SIFs of residual stress is the key for predicting fatigue crack growth rates of small cracks within shot peened residual stress field. However it is important that more evidence needs to be gathered from different materials and residual stress profiles.

In the current study, we have devised a simplified system, in which compressive residual stress fields are induced by indentation procedures in which the depth of compressive residual stress layer can be controlled by the indenting load. In addition a simplified through-thickness short fatigue crack (2D) geometry has been adopted, to enable SIFs for both applied stress and residual stress field to be calculated with precision. The aims of this study are to provide fundamental understanding of the effect of a residual stress distribution on short crack growth behaviour and to assess the applicability of conventional superposition methodology to short crack growth.

## **2. Material and experimental procedure**

The material used in this study is wrought Inconel 718, a widely used nickel-based superalloy. The nominal chemical composition in wt% for the alloy is given in Table 1. Specimens were extracted with their longitudinal direction along the radial direction from a disc forging supplied by Rolls-Royce plc. The material had received a heat-treatment procedure of solution heat treating at 1050°C for 1 hour, followed by air-cooling to 720°C, ageing for 8 hours, furnace cooling (1°C/min) to 620°C, ageing for 8 hours and finally air-cooling to room temperature. This heat treatment resulted in a coarse-grained structure with most of the grains in the size range 40-60  $\mu\text{m}$  although large grains up

to 90  $\mu\text{m}$  were occasionally observed. Room temperature tensile properties of the material investigated are given in Table 2. The stress-strain relationship measured was adopted for simulations of the residual stress fields generated by two indentation procedures using finite element (FE) modelling.

Fatigue crack propagation and threshold tests were carried out at room temperature using Single Edge Notch Bending (SENB) specimens of dimensions 20 (W)  $\times$  15 (B)  $\times$  100 (L)  $\text{mm}^3$  containing a notch of depth 2 mm. A computer-controlled Amsler Vibrophore was utilised to achieve automatic load reduction with the extension of the fatigue crack, while running at a frequency of approximately 80 Hz. The tests were performed at load ratios,  $R$  ( $R = P_{\min}/P_{\max}$ , where  $P_{\min}$  and  $P_{\max}$  are the minimum and maximum load applied over the fatigue cycle respectively), of 0.1 and 0.7 respectively. A constant- $R$  and decreasing- $\Delta K$  procedure [12] was followed until a growth rate,  $da/dN$ , of  $2 \times 10^{-8}$  mm/cycle was achieved. The closure stress intensity,  $K_{\text{cl}}$ , was approximated as the point of first deviation from linearity in the elastic compliance curve upon unloading [13]. An effective stress intensity range at threshold was estimated as  $(\Delta K_{\text{th}})_{\text{eff}} = K_{\text{max}} - K_{\text{cl}}$ .

Short through-thickness crack specimens were obtained by machining away the wake of long crack specimens, in which the cracks had propagated to the threshold at a stress ratio of 0.1, as shown schematically in Fig. 1. The depth of the short cracks was controlled to between 0.2 and 0.5 mm. Both sides of the specimens were also machined away and the thickness of the specimens was reduced to 10.0 mm, in order to obtain a straight crack front. These specimens were then stress relieved for 2 hrs at 700°C in a vacuum furnace to minimise any residual stress possibly caused by prior loading history and machining. Different preparation procedures were subsequently applied in order to prepare the samples with different stress fields. One set of samples were indented twice on the top surface with a spacing of 4 mm using a carbide cylinder of 8 mm diameter. The indentations are parallel to and have an equal distance from the crack. These specimens are denoted here by the term “2-indent”. An indentation load of 20 kN was selected to give an appropriate magnitude and size of residual stress field. The 4 mm spacing was selected because this is larger than the lateral extent of the plastic zone produced by the indentation. Hence residual stress is generated without strain hardening along the



crack plane. A second set of samples were indented once only on the top of the crack using the same indenter and load, as illustrated in (Fig.1b). These specimens are denoted here by the term “1-indent”. In this case, both residual stress and pre-strain were introduced along the crack plane. A third set of specimens was left as stress-relieved which provides a baseline of short crack growth rates. They are denoted here by the term “0-indent”. An ABAQUS package was used for the associated FE modelling.

Short fatigue crack growth tests were performed at room temperature for such “0-indent”, “1-indent” and “2-indent” specimens under constant amplitude loading in a four-point-bending configuration using an Instron 1273 servo-hydraulic test machine with load capacity of 10 kN.  $R$  ratios of 0.1 and 0.7, a frequency of 10 Hz and a sinusoidal waveform were used. During the test, the crack opening levels at different crack lengths, in all three sets of specimens were measured using the back-face strain compliance method as described previously [14].

Crack lengths were monitored by a d.c.p.d. (direct current potential drop) technique using in-house experimental calibrations and verified individually against the measurements of initial and final crack length. Note that the SIFs of all tests were calculated using the equations given by Tada et al [15] which applies to all values of  $a/W$  for four-point bending specimens.

Following the fatigue crack growth tests, the fracture surfaces that corresponded to short crack growth, and the near-threshold, Paris and high  $\Delta K$  regimes of the long fatigue crack growth were examined using an Hitachi S-4000 FEG-SEM operating in secondary electron mode with  $0^\circ$  tilt.

### **3. Results and discussion**

#### **3.1 Fatigue crack growth and threshold of long cracks**

Fatigue crack growth rates,  $da/dN$ , versus nominal stress intensity factor range,  $\Delta K$ , obtained for long cracks are shown in Fig.2. Both curves ( $R=0.1$  and  $0.7$ ) show regimes of near-threshold and stable crack growth. As expected, the long crack growth rates for a stress ratio of 0.7 are much higher than those for a stress ratio of 0.1 at a given SIF range value,  $\Delta K$ . The threshold SIF ranges were measured as 10.2 and 5.8  $\text{MPa}\sqrt{\text{m}}$  at  $R=0.1$  and  $R=0.7$ , respectively. The data are in good agreement

with the results obtained from other studies of similar alloys [16]. The macroscopic fracture surfaces for these two  $R$  ratios are shown in Fig. 3.

The observed effect of load ratio on near threshold fatigue crack growth is commonly attributed to the role of crack closure. In addition to any plasticity induced crack closure, a significant contribution also comes from roughness-induced closure. The fracture surface in the near threshold region features large, angular crystallographic facets, and is significantly rougher than the smooth transgranular morphology in the Paris region. The fracture surface appearance is dictated by underlying deformation mechanisms. Comparisons of fracture surface morphology are given in Fig. 4 for both  $R$  ratios and suggest a less pronounced tendency for crystallographic growth at a  $R$  ratio of 0.7. The crack opening stress intensity factor,  $K_{cl}$ , was measured to be approximately  $4.3\text{MPa}\sqrt{\text{m}}$  at  $R=0.1$ , from which it is deduced that the crack was closed for 42% of the total SIF range at threshold. It is desirable from a lifing point of view to derive an intrinsic fatigue crack growth resistance curve which is free of the effect of crack closure. Such intrinsic data are attempted in this study with the application of a high stress ratio of 0.7. Indeed no detectable closure (from back-face strain gauges) was observed even at threshold. The threshold value obtained ( $10.2 - 4.3 = 5.9\text{MPa}\sqrt{\text{m}}$ ) is closely similar to the effective stress intensity factor range,  $(\Delta K_{th})_{eff}$  (after deducting the closure portion), at  $R$  ratio of 0.1 ( $5.9\text{MPa}\sqrt{\text{m}}$ ). This suggests strongly that the fatigue crack growth  $da/dN$  versus  $\Delta K$  curve obtained at a  $R$  ratio of 0.7 is representative of an intrinsic  $\Delta K$  versus  $da/dN$  relationship.

### 3.2 Fatigue crack growth of short cracks

Fig. 5 shows short crack growth resistance curves for 0-indent specimens at stress ratios of 0.1 and 0.7. The long crack growth data obtained for this material at both stress ratios are also shown for comparison. At a stress ratio of 0.1, "typical" short crack growth behaviour is observed for short cracks free of residual stresses. With an initial applied  $\Delta K$  value of  $7\text{MPa}\sqrt{\text{m}}$  which is lower than the threshold value of long cracks at this stress ratio ( $\sim 10\text{MPa}\sqrt{\text{m}}$ ), the short crack initially grew from a growth rate indicated by the intrinsic (long-crack  $R = 0.7$ )  $da/dN$  versus  $\Delta K$  curve, and gradually deviated away and merged into the long crack growth curve ( $R=0.1$ ) as the crack length and applied  $\Delta K$  increase. This implies the crack opening behaviour goes through a transient from "fully open" to a

steady-state which is similar to that obtained for long cracks. Such behaviour reflects an extrinsic effect in reducing the driving force at the local crack tip. Another test started with a larger initial  $\Delta K$  value of  $\sim 10 \text{ MPa}\sqrt{\text{m}}$  ( $R=0.1$ ) also demonstrated a similar transition from the intrinsic crack growth curve to the long crack growth curve, however the fatigue crack growth rates are now much faster in general. It is not surprising to find that the short crack growth at  $R=0.7$  followed exactly the crack growth law of long cracks as the extrinsic contribution to fatigue crack growth resistance is absent in both cases.

### 3.3 Effects of residual stress on short fatigue crack growth

#### 3.3.1 Residual stress distributions caused by indentation

Due to very low X-ray diffraction intensity from the major phase in Inconel 718, it was impossible to use conventional X-ray diffraction to measure subsurface residual stresses. However elastic-plastic FE modelling was performed using the ABAQUS finite element package, to obtain the size of the plastic zone and the residual stress distribution resulting from the two indentation procedures. Due to the symmetry of the contacts, only half of the structure needs to be modelled. Note here that strain and stress distributions were only considered using 2-Dimensional plane-strain analysis only. The FE model was validated by measurements of the displacement of the indenter after indentation.

Fig. 6 demonstrates FE predictions of plastic zones after applying a 20 kN load for both “2-indent” and “1-indent” conditions. It can be seen that the plastic zone is approximately 2.5 mm in width and 2.1 mm in depth, and is fully contained by surrounding elastic material. With a 4 mm spacing between two indentations, referred as “2-indent”, the mode I crack plane is still within an elastic zone between the two plastic zones. On the crack path of the “1-indent” case together with the residual stress field generated, pre-straining also occurs within the plastic zone along the crack path. Fig. 7 gives a comparison of the residual stress profiles (mode I direction normal to the crack plane) along the depth direction (crack growth direction) for both cases as calculated by FEM and as a result of the proximity of the plastic zone achieved by the indentation. The plot shows that the maximum compressive stress occurs at the surface of the specimens that had been subjected to two indentations

and has a magnitude of approximately -300 MPa. The depth of the compressive layer is approximately 1.5 mm. For the “1-indent” case, the maximum compressive stress occurs sub-surface and has a magnitude of -636 MPa. The depth of the compressive zone is approximately 2.1 mm. It is expected that such variation in residual stress fields, although different in magnitude and depth, provide simplified models for cases that could occur for a shot peened surface where coverage of the surface is incomplete.

### 3.3.2 Short fatigue crack growth in 2-indent specimens

In Fig. 8, the short fatigue crack growth curves obtained for the indented specimens show different forms compared to those without indentation shown in Fig.5. At a stress ratio of 0.1, two tests were conducted with different initial  $\Delta K$  values. One test was started with an initial  $\Delta K$  of  $\sim 9$  MPa $\sqrt{m}$  (“2-indent\_1”). Under such an applied driving force the crack grew. However, crack growth rates were reduced, compared to the both “0-indent\_1” (initial  $\Delta K = \sim 7$  MPa $\sqrt{m}$ ) and “0-indent\_2” (initial  $\Delta K = \sim 10$  MPa $\sqrt{m}$ ) in Fig. 5. The slow growth region is found to correspond roughly to the depth of the compressive residual stress zone. When the crack length was longer than 1.5 mm (the point at which the residual stress is considered to become zero – see Fig. 7), crack growth rates accelerate and start to merge into crack growth rates for long fatigue cracks ( $R = 0.1$ ). Another indented specimen (“2-indent\_2”) was started with a much reduced initial  $\Delta K$  of 6 MPa $\sqrt{m}$ , which is close to the intrinsic threshold for this material. No crack extension was recorded after  $5 \times 10^5$  cycles. Then a load increasing procedure was applied until the crack started to propagate. Eventually at a  $\Delta K$  value of 9 MPa $\sqrt{m}$  crack growth occurs. From both experiments and in comparison to results from “0-indent” samples it can be concluded that a compressive residual stress can both reduce crack growth rates as well as to increase the “fatigue threshold” for short fatigue crack growth (from approximately 6 to 9 MPa $\sqrt{m}$ ).

At a high stress ratio of 0.7, any such effects of compressive residual stresses on short crack growth rates were not observed. The crack growth curve is found to be consistent with those of “0-indent” (short crack in the absence of residual stress), and long fatigue cracks ( $R=0.7$ ). This implies that the intrinsic fatigue crack growth resistance relationship obtained from growing long fatigue

cracks applies also for short through thickness fatigue cracks. The effect of residual stress can thus be described as an extrinsic closure factor. Note that the short fatigue cracks studied here are two-dimensional through-thickness cracks, in which the crack front covers a large number of grains (~150). This may not necessarily apply for the case of naturally self-initiated small surface cracks which tend to initiate at inclusion particles or voids, in regions of intense slip within large grains, or at weak interfaces. In these cases, metallurgical similitude will be expected to break down and local growth rates may no longer reflect an average taken over many grains.

From the results shown above, the propagation of short through-cracks in the presence of a compressive residual stress field can be summarised by the following points: (1) in the presence of compressive residual stress, short crack growth rates were reduced compared to those of the residual stress free specimens, at the same initial  $\Delta K$  value; (2) an additional driving force was needed to start short crack growth in a compressive residual stress field; (3) short crack growth tends to accelerate when the cracks grow out of the compressive residual stress zone; (4) the effects of a compressive residual stress field on short crack growth become less significant with increase of stress ratio. At a high stress ratio of 0.7, any beneficial effect of compressive residual stress is much reduced or absent.

### 3.3.3 Short fatigue crack growth under a conjoint effect of residual stress field and pre-strain

According to FE modelling, one indentation on top of the crack produces a higher and deeper compressive residual stress than that in the case of two indentations, one on either side of the crack, under the same indentation force 20kN. In addition strain hardening is expected within the plastic deformation zone beneath the indent, which is approximately 2 mm in depth (Fig. 7).

Fig. 9 shows a comparison between a “1-indent” and a “2-indent” specimen with a similar initial short crack length. Under an initial  $\Delta K$  of  $\sim 9 \text{ MPa}\sqrt{\text{m}}$ , “2-indent” grew, but an initial  $\Delta K$  of  $10 \text{ MPa}\sqrt{\text{m}}$  had to be applied for the “1-indent” to grow. Even with the increased initial  $\Delta K$ , the crack growth rates within the compressive stress and plastic deformation field were very low (most of the values are less than  $1 \times 10^{-6} \text{ mm/cycle}$ , and some of them are less than  $5 \times 10^{-7} \text{ mm/cycle}$ ). After a crack length of 2 mm (the depth of compressive residual stress and plastic zone induced by indentation), the crack growth rates increased sharply. Clearly the fatigue crack growth resistance was significantly

increased in the “1-indent” condition, presumably due to deeper and larger compressive residual stress. It is difficult to judge whether pre-strain has contributed to the increased resistance. However, it is likely that residual stress is the primary factor. Indeed a negligible influence of pre-strain on near threshold fatigue crack growth is confirmed, for example, by Al-Rubaie et al for a 7475-T7351 aluminum alloy [17].

### 3.4 Effects of residual stress on crack closure

Early investigation of plasticity-induced crack closure by Elber [18] has led to a general acceptance of the concept that there is a unique, intrinsic fatigue crack growth law, but the applied mechanical driving force can be reduced through various mechanisms, which give rise to different fatigue crack growth phenomena, e.g. fatigue crack growth of short cracks, effect of overload and effects of residual stress. Although the original concept of crack closure relates to physical contact of crack faces behind of the crack tip during unloading from peak load before reaching minimum load, it has been extended to include other factors that shield and reduce the effectiveness of the external mechanical driving force [19]. As a result  $K_{cl}$  has become a broad term. Measurement of crack closure is relatively straightforward but accurate estimation is often difficult as it is highly sensitive to the method applied. Here, from the observed fatigue crack growth resistance curves,  $K_{cl}$  values can be estimated for short cracks assuming the same growth rates result from the same effective stress intensity factor range. Results are given in Fig. 10. The SIF values resulting from the compressive residual stress are also provided for comparison. Note that the  $K_r$  values are calculated using a weight function method [20].

From Fig.10, it is found that the  $K_{cl}$  values of residual stress free short cracks (“0-indent”) increase from the  $K_{min}$  values and gradually stabilise at a level of approximately 5-6 MPa $\sqrt{m}$  with the advance of the cracks. It is noted that these short cracks are obtained by machining away the wake of long cracks which had grown to the threshold under  $R$  ratio of 0.1, and therefore had the smallest possible plastic zone size. They were also further stress relieved at 700°C for 2 hrs to minimise the residual stress ahead of, and in the wake of, the crack tip. Thus, at the beginning of the crack extension, no crack closure is expected and is deduced. The gradual build-up and eventual stabilising

of  $K_{cl}$  is likely to be mainly plasticity- induced, perhaps being attributed more to “compressive residual stress” ahead of the crack tip, (induced by unloading followed by reloading and plastically deforming the crack tip region, rather than to actual contact in the crack wake – noting its limited length here of 0.2 – 0.5 mm. This transient crack closure behaviour is commonly observed and is believed to contribute to abnormal short crack growth behaviour. For the “2-indent” samples,  $K_{cl}$  values of approximately  $4 \text{ MPa}\sqrt{\text{m}}$  are present at the very beginning of crack propagation, presumably caused by the additional compressive residual stress (induced by indentation) acting both ahead of the crack tip and on the crack wake. The  $K_{cl}$  values increase more rapidly than those in “0-indent” specimens with an increase in crack length. After reaching a peak value of approximately  $9\text{--}11 \text{ MPa}\sqrt{\text{m}}$ , the  $K_{cl}$  values reduce rapidly to those of “0-indent” specimens. This happens at a crack length corresponding roughly to the depth of the compressive residual stress layer. However, the  $K_{cl}$  values are always found to be below the magnitude of the absolute  $K_r$  values. Also,  $K_r$  seems to have no effect at all on  $K_{cl}$  when the cracks grow out of the compressive residual stress layer.

From the results shown above, it is evident that an additional "clamping force" is induced by the pre-existing compressive residual stress field. It may be inferred that both the residual stress along the plastic wake of the crack and in the plastic zone ahead of the crack contribute to the increase of  $K_{cl}$  values as contact of fracture surface can now be confirmed from the observation of a dark band on the fracture surface within the compressive residual stress layer (Fig. 11 ). A similar band is also observed at the near threshold area with the long crack growth specimens at a stress ratio of 0.1 (Fig. 3a). These dark bands have been confirmed to be associated with formation of an oxide film due to contact and rubbing of the fracture surfaces, as demonstrated by SEM micrograph of the oxide film on top of the fracture surface (Fig.12) and qualitative EDX analysis. The  $K_{cl}$  values reduce to the level of that of the residual stress free specimens immediately after penetrating through the compressive residual stress layer, which suggests that the stress state ahead of the crack tip is important. Here it is deduced that closure in the crack wake alone cannot affect the effective driving force. Similar observations were also made by Kang et al [21] and other researchers [22], where they imply “partial crack opening” (the crack tip opens while the wake of the crack still remains in contact) occurs when fatigue cracks

grows through a transition region from residual compression to residual tension. The  $K$  value associated with opening at the crack tip,  $K_{\text{part.op}}$ , is far below that at the crack wake, the conventional  $K_{\text{op}}$ . They found that growth behaviour is well explained by using  $K_{\text{part.op}}$  rather than  $K_{\text{op}}$ , in a  $\Delta K_{\text{eff}}$  approach.

### 3.5 The applicability of $K_r$ in evaluating short crack propagation in a compressive residual stress field

Typical approaches to take account of the influence of residual stress on fatigue crack growth always seem to involve the calculation of a stress intensity factor associated with a pre-existing residual stress field,  $K_r$ . This is then superimposed onto the stress intensity factor resulting from the applied load which could either be rationalised by an “effective stress ratio”, or different levels of crack closure. Using  $K_r$  and its superposition offers a simple approach which has found success especially for long fatigue crack growth and for a residual stress field distributed over a long distance [23] or through a compressive residual stress field [24]. However there are indeed complications. One particular situation noted here is when a crack is immersed in a stress field where the sign changes, and with the tip located in the tensile zone. The investigation of short fatigue crack growth within a short range compressive residual stress imposes challenges from both experiment and analysis points of view. On one hand the absolute  $K_r$  is comparable to, or even higher than, the external peak applied stress, and on the other hand the magnitude of residual stress changes sharply. Indeed  $K_r$  can be shown to fail to describe the observed crack growth behaviour in the current study by considering, for example the “2-indent” condition when the crack grew under an initial  $\Delta K$  of  $\sim 9 \text{ MPa}\sqrt{\text{m}}$  ( $R=0.1$ ) and the corresponding  $K_r$  value is  $\sim 10 \text{ MPa}\sqrt{\text{m}}$ . Based on the superposition principle there is no tensile component within the full load range and crack growth should not occur. Further, when cracks grow out of the compressive residual stress field, no effect of  $K_r$  is found on fatigue crack growth rates here, whereas rather large negative values of  $K_r$  are still obtained from weight function calculations. Therefore it can be concluded that the influence of a compressive residual stress field would be overestimated using  $K_r$  and the superposition methodology. This is in accordance with the observation of Wilks [25] who demonstrated that the stress intensity factor of residual stress may be overestimated



when a sharp gradient exists in the residual stress field and partial crack opening occurs. A calculation using a dislocation density method instead of the traditional weight function method showed that the  $K_r$  value for such a case was close to zero. Kang [21] also found partial crack opening for long crack growth in the transition zone from residual compression to residual tension in a welding induced residual stress field. A  $K_r$  based analysis, where the  $K_r$  value was derived from weight function calculations, was also found to be unacceptable in his study also. In practice, the residual stresses due to shot peening and other mechanical surface treatments have both very high magnitude and sharp gradients. Partial opening of a crack may occur. In addition, due to the high amplitude of the residual stress, relaxation of residual stress may happen due to the service loading even before a crack starts, and such changes need to be accounted for in the analysis.

The crack closure approach is certainly of merit here. The quantification of residual stress on crack closure,  $K_{cl}$ , however, is complicated and cannot be estimated by an effective stress ratio. Further investigations both through numerical analyses and experiments are necessary.

#### 4. Conclusions

Short fatigue crack growth through compressive residual stress fields induced by indentation procedures was investigated in the present study with a focus on near threshold crack growth. The applicability of traditional superposition of stress intensity factors of residual stress and external applied stress range was examined. The following conclusions can be made:

The fatigue threshold for long cracks was found to be 5.9 and 10.1  $\text{MPa}\sqrt{\text{m}}$  under the stress ratios of 0.7 and 0.1 respectively for the alloy investigated. This difference has been deduced to be due to significant crack closure present at the stress ratio of 0.1, deriving from potential additional crack closure mechanisms. A stress ratio of 0.7 is sufficient to fully open the fatigue crack throughout the fatigue crack growth regimes.

In the absence of residual stress, at a given stress ratio, short fatigue cracks start to grow at a growth rate suggested by the intrinsic fatigue crack growth resistance curve. As the short crack grows, its growth rates eventually merge with the long crack growth curve for the given stress ratio. Different

transient growth behaviour may be exhibited according to the initial  $\Delta K$  value. The intrinsic threshold value obtained for the long fatigue cracks was observed to be applicable to that for the through-thickness short cracks of depth 0.2-0.4 mm.

An imposed compressive residual stress has a profound influence on the growth of short fatigue cracks when they are contained in the compressive residual stress field. Both increase of fatigue threshold and decrease in fatigue crack growth rates are observed, comparing to those of short cracks free of residual stress. Immediately after the short cracks grow out of compressive residual stress layer, their crack growth rates return to normal despite negative SIFs calculated from the residual stress field.

The influence of compressive residual stress field on the growth of short cracks reduces with an increase of stress ratio. At a stress ratio of 0.7, little effect of residual stress was observed.

When using an "effective stress intensity range" concept to explain the growth behaviour of the short fatigue crack in the compressive residual stress field, the applied weight function solution yields conservative values of stress intensity factor of the residual stress field,  $K_r$ , suggesting this common approach used for long fatigue cracks may not be appropriate for short fatigue cracks.

**Acknowledgements:**

The authors are thankful for the support of Rolls-Royce plc. in providing of the materials. The assistance by Dr. KH Wang, previously a Ph.D student in School of Mechanical Engineering at Birmingham University, in the FE analysis is acknowledged.

**References:**

- [1] Torres MAS, Voorwald HJC. An evaluation of shot peening, residual stress and stress relaxation on the fatigue life of AISI4340 steel. *Int J of Fatigue* 2002;24:877-886.
- [2] Rios de Los ER, Walley A, Milan MT, Hammersley G. Fatigue crack initiation and propagation on shot-peened surface in A316 stainless steel. *Int J Fatigue* 1995;17:493-9.
- [3] Parker AP. Stress intensity factors, crack profiles, and fatigue crack growth rates in residual stress fields. Throop J, Reemsnyder H, editors. *Residual stress effects in fatigue*, ASTM STP 776, Pennsylvania ASTM International; 1982, p. 13-31.
- [4] Walker K. The effect of stress ratio during crack propagation and fatigue for 2024-T3 and 7075-T6 aluminum. Rosenfeld M editor. *Effects of Environment and Complex Load History for Fatigue Life*, ASTM STP 462, Pennsylvania ASTM International; 1970, p. 1-14.
- [5] Elber W. The significance of fatigue crack closure, damage tolerance in aircraft structures. Rosenfeld M, editor. *Damage Tolerance in Aircraft Structures*, ASTM STP486-EB, Pennsylvania ASTM International; 1971, p. 230-42.
- [6] Braid JEM. *Fatigue Crack Propagation in Residual Stress Field*, Thesis of the University of Cambridge; 1982.
- [7] Wu XR, Carlsson AJ. *Weight Functions and Stress Intensity Factors Solutions*, Pergamon Press; 1991
- [8] Knott JF, in *Proceedings of the 4<sup>th</sup> International Conference on Numerical Methods in Fracture Mechanics*, 1987, p.607-625.
- [9] Beghini M, Bertini L. Fatigue crack propagation through residual stress fields with closure phenomena, *Eng Fract Mech* 1990;36:379-387.
- [10] Lacarac V, Smith DJ, Pavier MJ, Priest M. Fatigue crack growth from plain and cold expanded holes in aluminium alloys. *Int J Fatigue* 2000;22:189-203
- [11] Gao YK, Wu XR. Experimental investigation and fatigue life prediction for 7475-T7351 aluminum alloy with and without shot peening-induced residual stresses. *Acta Mat* 2011;59: 3737-47.

- [12] British standard DD 186:1991
- [13] Suresh S. Fatigue of Materials. Cambridge University Press; 1991
- [14] Ray SK, Grandt Jr AF. Comparison of methods for measuring fatigue crack closure in a thick specimen. Newman Jr JC, Elber W, editors. Mechanics of Fatigue Crack Closure, ASTM STP 982, Philadelphia ASTM International; 1988, p.197-213.
- [15] Tada H, Paris PC, Irwin GR. Stress analysis of cracks handbook, 2<sup>nd</sup> ed. ASME Press; 1985, p.2.2 and 2.14.
- [16] Mercer C, Soboyejo ABO, Soboyejo WO. Micromechanisms of fatigue crack growth in a forged Inconel 718 nickel-based superalloy. Mater Sci Eng 1999;A270:308-322.
- [17] Al-Rubaie KS, Barroso EKL, Godefroid LB. Fatigue crack growth analysis of pre-strained 7475-T7351 aluminum alloy. Int J Fatigue 2006;28:934-42.
- [18] Elber W. Fatigue crack closure under cyclic tension. Eng Fract Mech 1970;2:37-44.
- [19] Ritchie RO. Mechanisms of fatigue crack propagation in ductile and brittle solids. Int J Fract 1999;100:55-83.
- [20] Tada H, Paris PC. The stress intensity factor for a crack perpendicular to the welding bead. Int J Fract 1983;21:279-84.
- [21] Kang KJ, Song JH, Earmme YY. Fatigue crack growth and closure behaviour through a compressive residual stress. Fatigue Fract Eng Mater Struct 1990;13:1-13.
- [22] Beghini M, Bertini L. Fatigue crack propagation through residual stress fields with closure phenomena. Eng Fract Mech 1990;36:379-384.
- [23] Ohta A, McEvily AJ, Suzuki N. Fatigue crack propagation in a tensile residual stress field under a two-step programmed test. Int J Fatigue 1993;15:9-12.
- [24] Kang KJ, Song JH, Earmme YY. Fatigue crack growth and closure through a tensile residual stress field under compressive applied load. Fatigue Fract Eng Mater Struct 1989;12:363-376.
- [25] Wilks MDB, Nowell D, Hills DA. The evaluation of stress intensity factors for plane cracks in residual stress field. J Strain Analysis 1993;28:145-52.

**Figure Captions:**

Figure 1. Schematic of indentation to induce compressive residual stress. (a) Two indents at both sides of the crack and (b) one indent on top of the crack.

Figure 2. Long fatigue crack growth resistance curves, obtained under two stress ratios ( $R=0.1$ ,  $R=0.7$ )

Figure 3. Typical fracture surface appearance (long crack) after fatigue threshold and fatigue crack propagation testing. (a)  $R=0.1$  and (b)  $R=0.7$

Figure 4. SEM micrographs showing the fracture surface morphology observed at a stress ratio of 0.1 (a) near threshold region and (b)  $\Delta K \approx 23.2 \text{ MPa}\sqrt{\text{m}}$ ; and at a stress ratio of 0.7 (c) near threshold region and (d)  $\Delta K \approx 15.8 \text{ MPa}\sqrt{\text{m}}$ . Note that the crack propagation direction is from left to right in all cases.

Figure 5. Fatigue crack growth resistance curves of the short fatigue cracks without residual stress field at stress ratios of 0.1 and 0.7. Note that the long crack data are also shown as solid line ( $R=0.1$ ) and dashed line ( $R=0.7$ ) for comparison.

Figure 6. Contours of equivalent plastic strain after unloading from “2-indents” (a), and “1-indent” indentation with an applied load of 20 kN.

Figure 7. FEM predicted residual stress distributions along the crack plane resulting from the different indentation procedures.

Figure 8. Fatigue crack growth resistance curves of the short fatigue cracks within a residual stress field induced by two indentations away from the crack.

Figure 9. Fatigue crack growth resistance curves of the short fatigue cracks within a residual stress field induced by one indentation only on top of the crack, compared with two indents parallel to the crack (but at 4 mm distance apart – see text).

Figure 10. Comparison of crack closure,  $K_{cl}$  between 0-indent and 2-indents tests. The Residual stress intensity values,  $K_r$ , for the 2-indents samples are shown in reversed values for comparison.

Figure 11. Comparison of the fracture surface appearance between a residual stress free specimen (left) and a indented specimen (right). A dark band formed inside the compressive residual stress layer.

Figure 12. SEM micrograph showing cracked oxide film in the dark bands of both indented and long crack specimens ( $R=0.1$ ).

<b>Fe</b>	<b>Cr</b>	<b>Co</b>	<b>Nb</b>	<b>Mo</b>	<b>Ti</b>	<b>Al</b>	<b>C</b>
20	19	0.5	5.3	3	1	0.6	0.045

**Table 1.** Composition (weight percent) of Inconel 718, Balance Ni

<b>E (GPa)</b>	<b><math>\sigma_{0.2}</math> (MPa)</b>	<b>UTS (MPa)</b>	<b>Elongation (%)</b>
198	1097	1303	21.7

**Table 2.** Tensile properties of Inconel 718 at room temperature

Fig. 1.

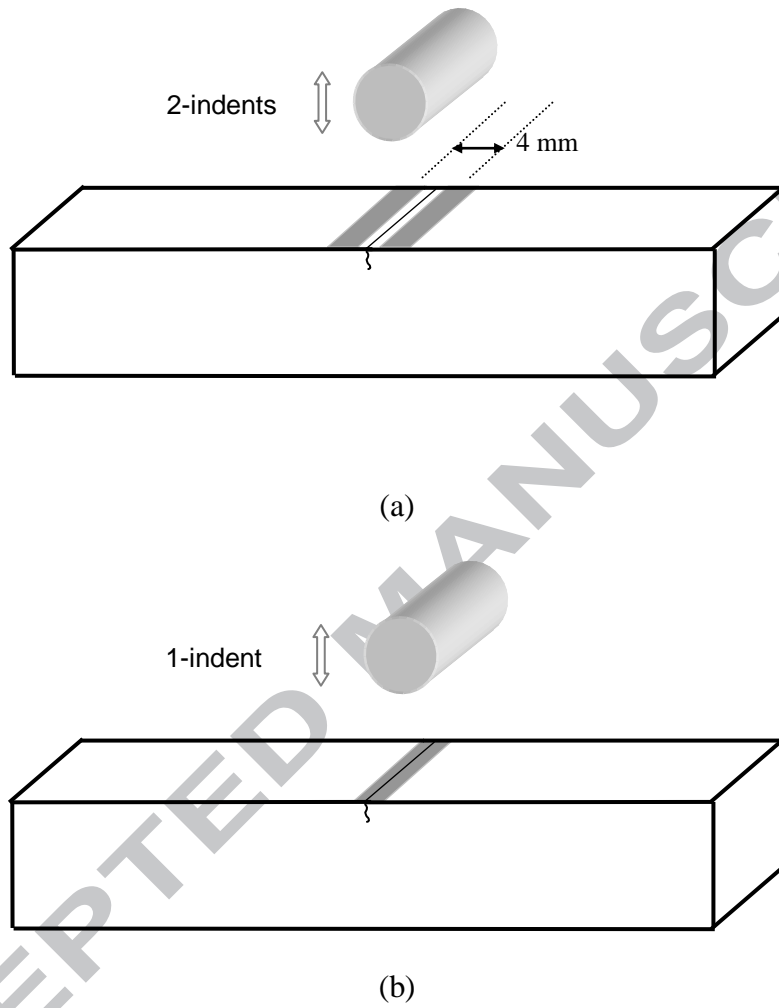


Fig. 2

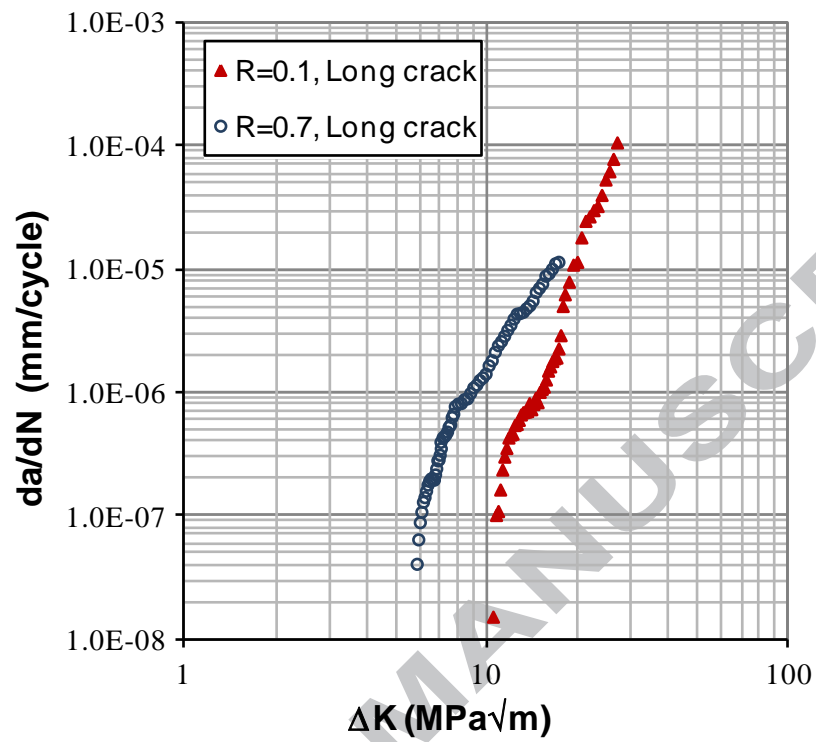


Fig. 3

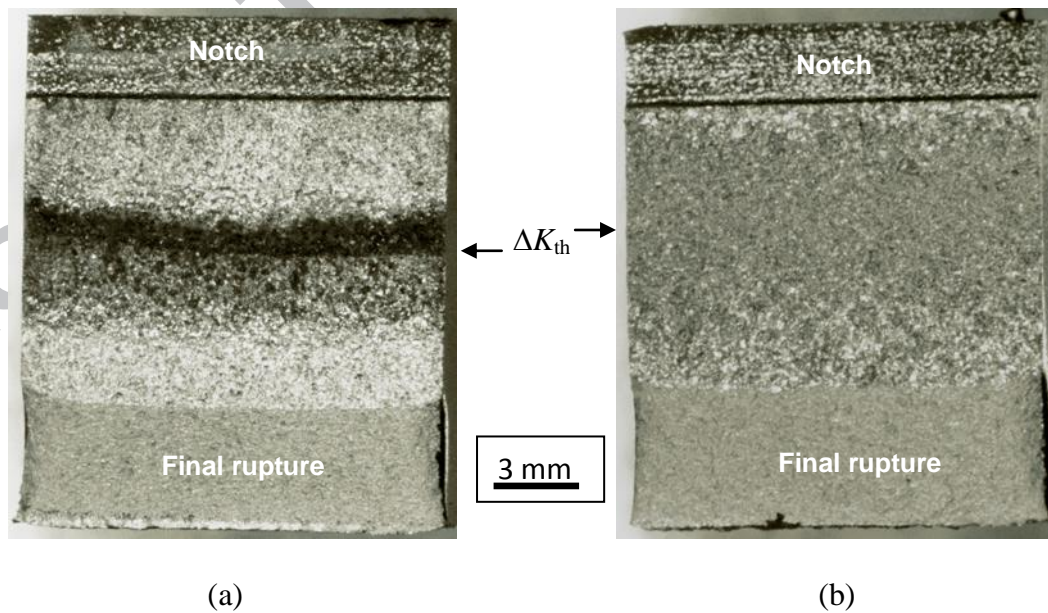




Fig. 4

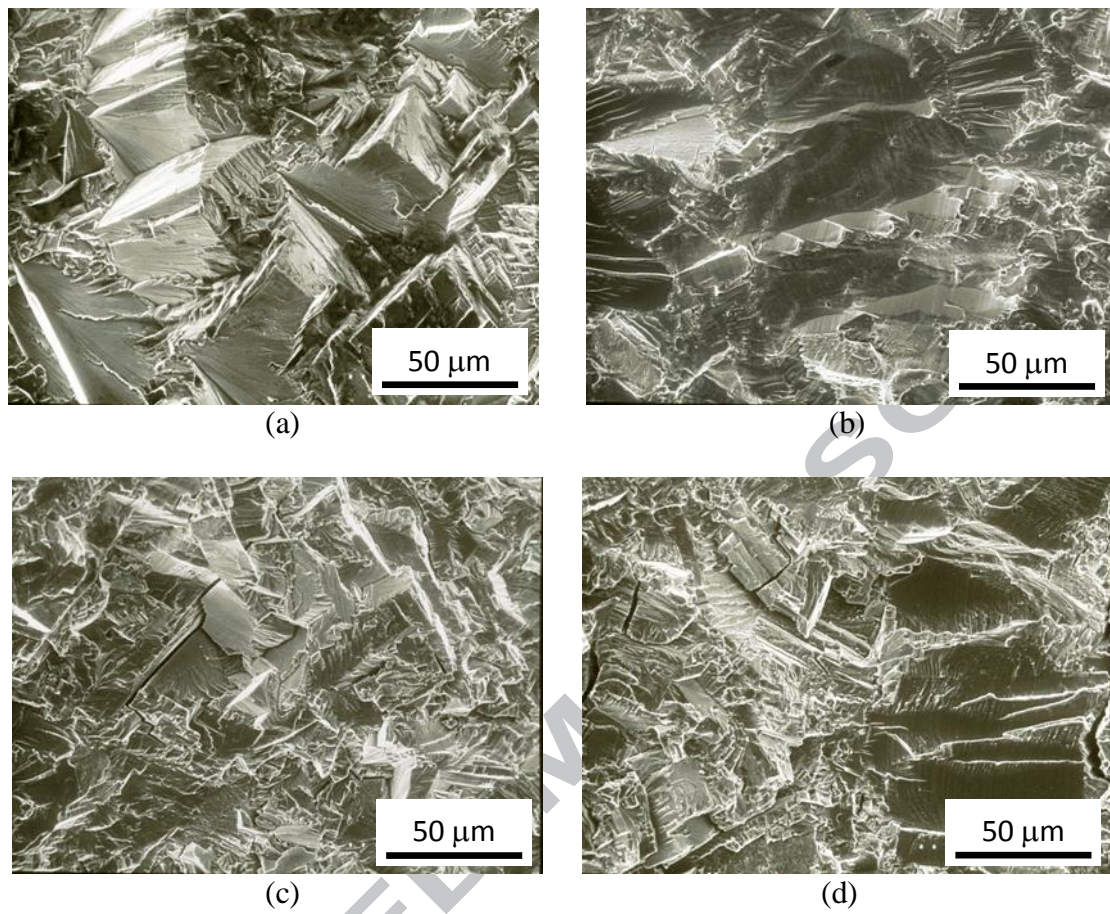


Fig. 5

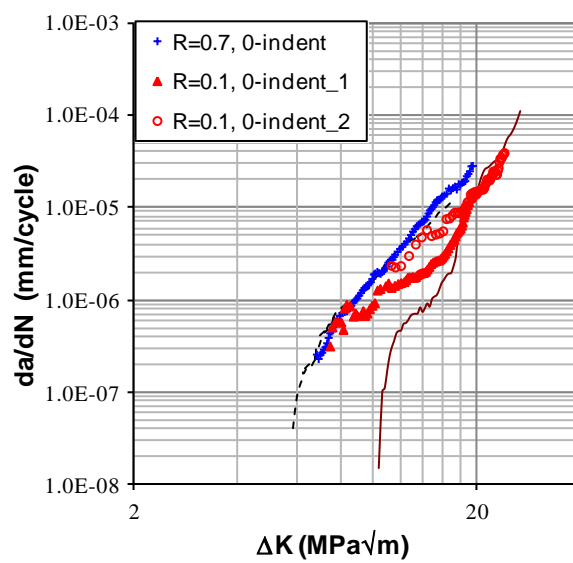
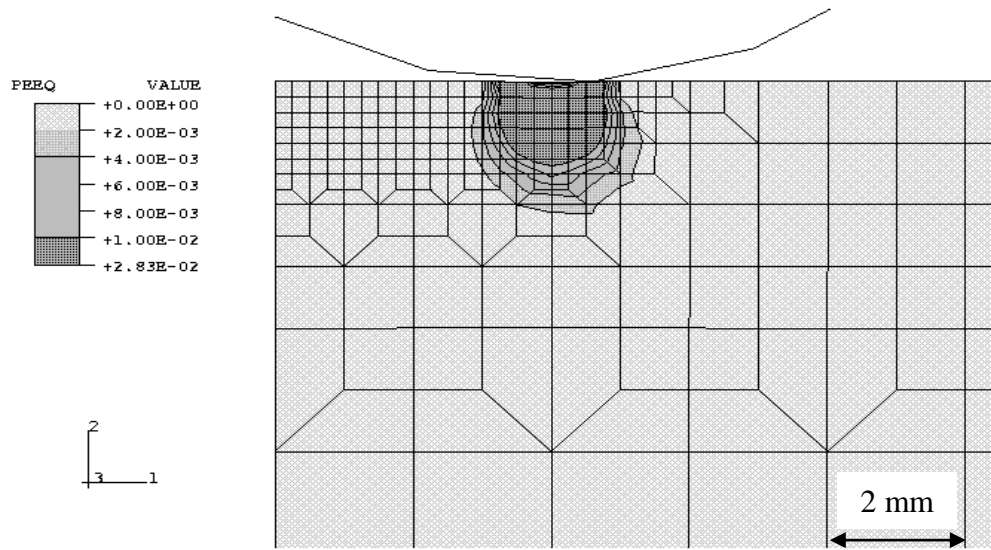
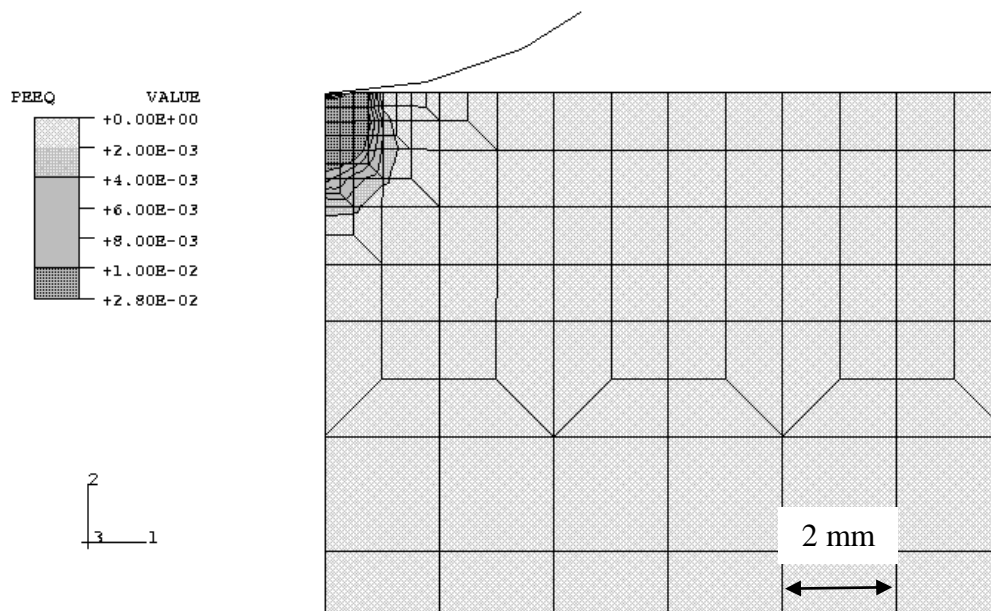


Fig. 6



(a)



(b)

Fig. 7

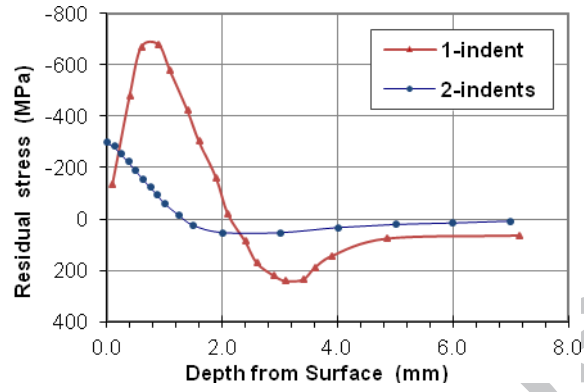


Fig. 8

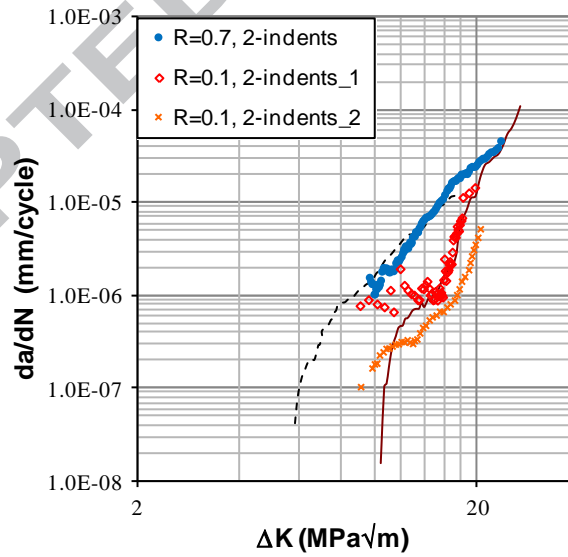


Fig. 9

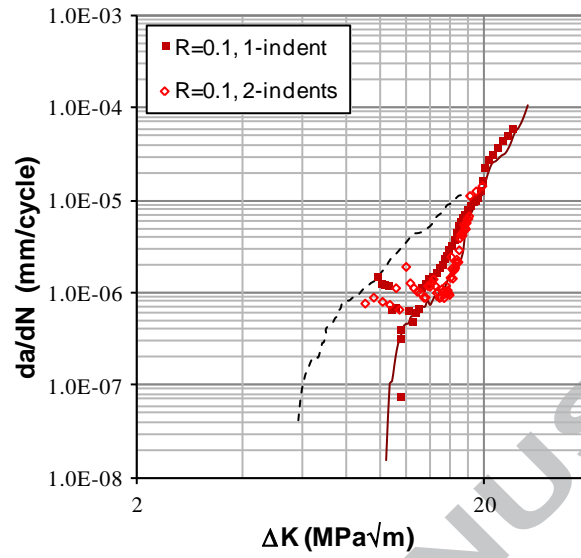


Fig. 10

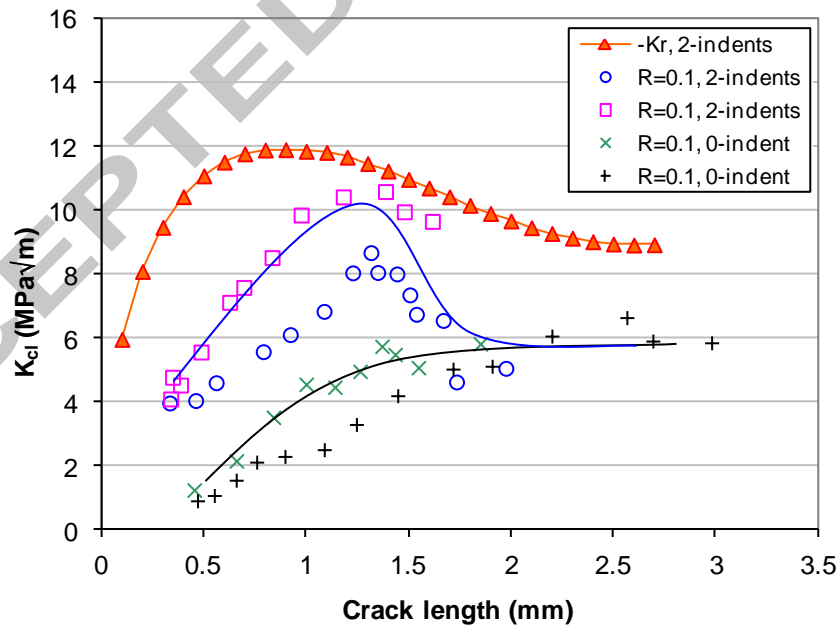


Fig. 11

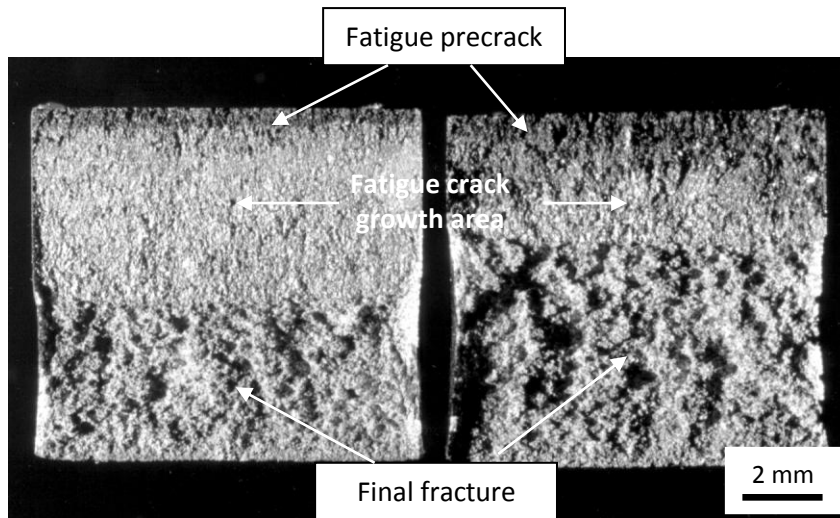
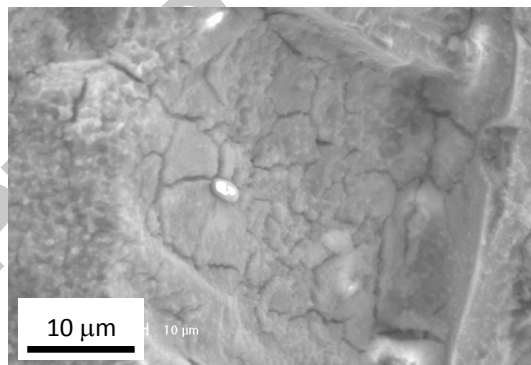


Fig.12



**Highlights:**

Fatigue crack growth behaviour of short through-thickness cracks (0.2-0.4 mm) in a nickel-based superalloy was investigated at room temperature.

By varying load, location and number of indentations, different residual stress fields can be conveniently introduced onto short cracks.

Fatigue crack growth behaviour of short through-thickness fatigue cracks can be described fully by a closure concept.

The influence of compressive residual stress field on short through-thickness cracks cannot be appropriately estimated by residual stress intensity factor,  $K_r$ , using a weight function method.

ACCEPTED MANUSCRIPT